33rd Annual International Conference of the IEEE EMBS
Boston, Massachusetts USA, August 30 - September 3, 2011

Simultaneous Segmentation and Inhomogeneity Correction in Magnetic Resonance Images

Yue Li, Julie Hoover-Fong, John A. Carrino and Susumu Mori

Abstract— **In Magnetic Resonance Imaging (MRI), intensity inhomogeneity has been an issue affecting the quality of post processing. In this paper, we present a simultaneous segmentation and inhomogeneity correction (IC) method based on active contour algorithm. It uses a generative model which is a modified Mumford-Shah functional proposed by Chan and Vese. The piecewise constant image model in the functional is multiplied by an underlying intensity inhomogeneity field. The inhomogeneity field and piecewise constant function are jointly estimated in an iterative way including solving the associated contour evolution equation and updating corresponding parameters. The algorithm is implemented using the level set framework. Test on MRI leg data shows our method achieves more accurate segmentation and IC results than other related methods in MR images with strong intensity inhomogeneity.**

I. INTRODUCTION

Magnetic Resonance Imaging (MRI) is a popular tool for exploring anatomy of human body and diagnosing diseases. In the past decades, numerous computerized image processing methods have been developed to facilitate the understanding of MR images. However, intensity inhomogeneity has been an issue affecting the quality of post processing. It could be caused by spatially varying sensitivity of radio frequency (RF) imaging coils, magnetic permeability and dielectric property of imaged objects, rendering smoothly changing bright and dark regions in the magnitude images. It becomes severer in the cases of large field of view (FOV) such as whole body imaging. Under the scenario, both anatomy and inhomogeneity field contribute to the intensity value changes across the images. Without inhomogeneity correction (IC), the intensity-driven segmentation/registration methods cannot distinguish the effects of these two components and will fail.

Intensity inhomogeneity can be partly alleviated by prospective shimming techniques, while the object-dependent effect requires more retrospective efforts. To do so, usually an IC step is inserted into the early stage of processing pipeline to accommodate the remaining steps. The main task of a IC method is to separate the effect of anatomical component of intensity change from inhomogeneity to make an accurate inhomogeneity estimation. Filtering based methods have been designed to extract the low frequency components of images as inhomogeneity[1], [2], but the transitions of anatomy and inhomogeneity can't be simply separated by their spatial frequency components. Due to the coupled nature of the problem, it's appealing to do segmentation and intensity inhomogeneity field estimation under an unified framework to make both of them more effective. In fact, many IC methods are designed in this way. For example, the segmentation methods based on maximum likelihood (ML) or maximum $aposteriori$ (MAP) type parametric probability distribution estimations have been adapted to take account of intensity inhomogeneity[3], [4], [5]. However, they are sensitive to initial values and require manual interactions due to the high dimensionality of parameter space. Another example is the widely used N3 [6] method which tries to sharpen the peaks in the histogram of (log-transformed) intensity values of different tissues that have been blurred by inhomogeneity. Although it doesn't directly result in a segmentation, it's aimed to make a more accurate classification of tissues based on intensity. However, the above methods do not exploit any geometric information in the image such as the pixel connectness. On the other hand, active contour [7] has been successfully used for segmentation in medical images. The advantage of active contour based methods is they exploit both intensity and geometric information of the images to be segmented.

To this end, a generative model of MR image accommodating both anatomical and inhomogeneity information is proposed in this paper. It's a modified version of Chan-Vese's(C-V) [8] Mumford-Shah(M-S) functional. Different from their method, which models images as piecewise constant functions, the proposed model takes into account the inhomogeneity by multiplying the image a smoothly changing field. The boundaries and the field are jointely estimated, using the level set framework. [9] We demonstrate on a dataset that our method outperforms the original C-V's or M-S functional, as while as the N3 pluses M-S method.

II. METHOD

A. Mumford-Shah functional and Level Sets Based Segmentation

In medical image segmentation, level set, or geometric active contour based methods have been paid much attention to. Particularly, C-V's method and its variations have been reported in multiple segmentation tasks. It segments a

This work was partially supported by the National Marfan Foundation and NIH P41RR15241.

Y. Li is with the Department of Biomedical Engineering, Johns Hopkins University School of Medicine, Baltimore, MD 21287, USA yueli.bme@gmail.com

J. Hoover-Fong is with McKusick-Nathans Institute of Genetic Medicine, Department of Pediatrics, Johns Hopkins University School of Medicine, Baltimore, MD 21287, USA jhoover2@jhmi.edu

J.A. Carrino and S. Mori are with the Russell H. Morgan Department of Radiology and Radiological Science, Johns Hopkins University School of Medicine, Baltimore, MD 21287, USA jcarrin2@jhmi.edu susumu@mri.jhu.edu

bimodal image by minimizing a simplified Mumford-Shah functional[10]:

$$F(\vec{C}, c_1, c_2) = \lambda_1 \int_{inside(\vec{C})} (I(x) - c_1)^2 dx + \lambda_2 \int_{outside(\vec{C})} (I(x) - c_2)^2 dx + \mu \cdot \text{Length}(\vec{C}) \quad (1)$$

where x is the spatial variable, c_1 and c_2 are the mean values of intensity inside and outside the closed curve $\vec{C}$ which is the boundary of segmented region. λ_1, λ_2 and μ are user defined weighting factors. The first two terms ask for the fidelity of the image to a regionwise constant valued function, with the region enclosed by $\vec{C}$. The function values inside/outside the regions are defined by c_1 and c_2 respectively. The third term asks smoothness of the curve.

This formula suits the images in which there are two kinds of regions(tissues) with different constant intensity values in each one and smooth boundary. The model for images with more than two distinct constant-valued regions can be found in [11], [12].

In [10], the problem is solved by an iterative scheme. In each iteration, first with c_1 and c_2 fixed, $\vec{C}$ evolves by gradient descent, and then, c_1 and c_2 are updated according to the new $\vec{C}$ position. Steps repeat until convergence. In the curve evolution step, the gradient flow can be written as:

$$\vec{C}_t = \lambda_2 (I(x - c_2))^2 \vec{N} - \lambda_1 (I(x) - c_1)^2 \vec{N} - \mu \cdot \kappa(x) \vec{N} \quad (2)$$

where κ and $\vec{N}$ are the curvature and normal direction of $\vec{C}$. This curve evolution is solved using the level set framework, where $\vec{C}$ is implicitly represented as the zero level set of a function $\phi(x)$ such that $\vec{C} = \{x, \phi(x) = 0\}$. $\phi(x)$ is usually initialized to be the signed distance function of $\vec{C}$[9]. Under this framework, (2) can be converted to the equivalent problem:

$$\phi(x)_t = -(\lambda_2 (I(x) - c_2)^2 - \lambda_1 (I(x) - c_1)^2 - \mu \cdot \kappa(x)) |\nabla \phi| \quad (3)$$

where κ is the curvature of ϕ: $\kappa = \nabla \cdot \frac{\nabla \phi}{|\nabla \phi|}$. After updating ϕ, the new position of $\vec{C}$ can be retrieved by extracting the zero level set of ϕ.

Different from the original M-S's functional, the regionwise constant model of C-V's method takes into account the regional means c_1 and c_2 as global properties and is less sensitive to initial condition. But it's not plausible when intensity inhomogeneity exists, and additional treatment is needed, which will be discussed next.

B. Integrating Inhomogeneity Field into C-V's Model

A few models have been used to describe the effect of intensity inhomogeneity in MRI. A widely used one considers it as a smooth field (b) multiplied to the inhomogeneity-free image then pluses noise[13]:

$$I(x) = I_h(x) \times b(x) + n(x) \quad (4)$$

where I_h is an ideal image free of inhomogeneity and n is a noise field[13].

We modified (1) for images with inhomogeneity fields as:

$$F(\vec{C}, c_1, c_2, b) = \lambda_1 \int_{inside\vec{C}} (I(x) - c_1 b(x))^2 dx + \lambda_2 \int_{outside\vec{C}} (I(x) - c_2 b(x))^2 dx + \mu \cdot \text{Length}(\vec{C}) \quad (5)$$

In this formula, c_1 and c_2 are the regional means in the inhomogeneity free I_h and then I_h is corrected by inhomogeneity field b to approximate the measured intensity value I. The gradient flow of (5) with fixed c_1, c_2 and b is:

$$\vec{C}_t = \lambda_2 (I(x) - c_2 b(x))^2 \vec{N} - \lambda_1 (I(x) - c_1 b(x))^2 \vec{N} - \mu \cdot \kappa(x) \vec{N} \quad (6)$$

and the corresponding level set equation becomes:

$$\phi(x)_t = -(\lambda_2 (I(x) - c_2 b(x))^2 - \lambda_1 (I(x) - c_1 b(x))^2 - \mu \cdot \kappa(x)) |\nabla \phi| \quad (7)$$

We propose the following iterative algorithm (see Algorithm 1) for simultaneous segmentation and IC (superscripts indicate number of iteration).

In each iteration, b is parameterized as a polynomial of x and is estimated by minimizing the cost:

$$b^{(i)} = \underset{b}{\text{argmin}} \lambda_1 \int_{inside(\vec{C}^{(i)})} (I(x) - c_1^{(i)} b(x))^2 dx + \lambda_2 \int_{outside(\vec{C}^{(i)})} (I(x) - c_2^{(i)} b(x))^2 dx \quad (8)$$

Algorithm 1 Simultaneous segmentation and inhomogeneity correction

1. Initialization: compute $c_1^{(0)}$, $c_2^{(0)}$, $b^{(0)}(x)$ and $\phi^{(0)}(x)$ from $\vec{C}^{(0)}$

Repeat step 2-4 until convergence.
For the ith iteration:
2. Update level set function corresponding to $\vec{C}^{(i-1)}$ using (7) with values of $c_1^{(i-1)}$, $c_2^{(i-1)}$ and $b^{(i-1)}$;
3. Update to $c_1^{(i)}$, $c_2^{(i)}$ with $\vec{C}^{(i)}$ and $b^{(i-1)}$;
4. Update to $b^{(i)}$ by minimizing the cost function (8)

A possible alternate to this is to use original M-S model, which models a image as a regionwise smooth instead of constant-valued function. But the lacking of the global properties in the constraints makes the method sensitive to initial condition and thus less robust. The comparison of our proposed and original M-S method will be shown in the following section.

Initial condition sometimes becomes critical to results of many curve evolution based methods. Here in our testing, we chose different kinds of initial curves for our method and original M-S functional approach. For original C-V and our method, arrays of squares were chosen as initial curves, while

for original M-S model, initial curve is a single rectangle. The reason is C-V's method allows numerous separated initial curves because the initially isolated regions are still "connected" via the regional means (c_1 and c_2). However, in the original M-S model, the piecewise smooth functions estimated in isolated regions are not related unless they are topologically connected. Therefore, for segmenting single connected objects, the number of initial curves shouldn't be large, and is usually one to keep the region(s) as connected as possible. There are two reasons of choosing arrays of squares chosen as initial curves: first, theoretically speaking, the estimated inhomogeneity field is independent to anatomy. Therefore, "uniformly" distributed internal and external regions at the beginning can eliminate the influence of anatomy most effectively and make the estimated inhomogeneity field more accurate. Second, for a "dense" distributed initial curve set, the true boundary should be close to part of it, method will be faster to reach global optimal.

III. EXPERIMENT

The proposed method was tested in a segmentation task to extract muscle region in a T1 weighted leg MRI data set. The dataset is with strong RF coil sensitivity inhomogeneity (one slice shown in Fig. 1(a) as an example). The image was acquired on a male subject by a Siemens Triotim 3T scanner, with gradient echo / inverse recovery sequence and body coil. The matrix size of axial slice of is 256x144 with pixel size 0.88mmx1.5mm.

First the entire leg region was extracted from background by a simple gray level thresholding. All the methods tested were performed in this region which contains fat (outer) and muscle (inner, surrounding the thighbone) and is suitable for bimodal segmentation task.

Four methods were tested. M1: C-V's method, with $\lambda_1 = \lambda_2 = 1$ and $\mu = 0.03$. M2: our method, which parameterizes the inhomogeneity field b as a 2D third order polynomial, other parameters and initialization are the same as in M1. Initial curves for M1 and M2 are the outlines of evenly spaced arrays of squares (as in Fig. 1(a)), size is 10x10 pixel (distance between neighboring squares is the same as their size), please note that although the initial regions are topologically isolated, the evolution of their boundaries are coupled because they share the same the regional mean values (c_1 and c_2) as global properties. M3: method in [11], which optimizes the original M-S functional[8], it models ideal images as regionwise smooth functions instead of regionwise-constant ones, so it could handle image with intensity inhomogeneity. Parameter: $\alpha = 200$, $\beta = 1$, $\gamma = 0.03$ (see the definitions in [11]), initial curve is the outline of a single rectangle as in Fig. 1(b), the reason is the original M-S functional doesn't carry any global properties as C-V's version and if the initial regions are isolated, the curves will not affect each other until they merge. M4: a two-step method, first a non-segmentation-associated IC method N3[6] was performed on original image and then M3 was applied to the output image. Other parameters and initial condition are the same as M3 except $\alpha = 500$ for heavier spatially variability constraint of approximated image. Curve evolution was implemented by level set method in matlab. N3 IC is downloaded as an *itk*(http://www.itk.org) class [14]. All parameter are selected by trial and error to maximize the performances.

	Sensitivity	Accuracy	Specificity
M2	0.9523	0.9704	0.9832
M3	0.9304	0.9649	0.9893
M4	0.8582	0.9319	0.9841

TABLE I
PERFORMANCE COMPARISON OF THE METHODS

IV. RESULT

Two slices (named $S1$ and $S2$) in the tested dataset are shown to demonstrate the performance of different methods. As in Fig. 1(c) as an example, M1 failed to detect boundary of muscle in dark area in all slices because of intensity inhomogeneity. M2 succeeded in both images in Fig. 1(d) and Fig. 1(l). The calculated inhomogeneity fields (Fig. 1(f) and 1(n)) indicate good approximation of inhomogeneity patterns each slice respectively. The "quotient images" (underlying images in Fig. 1(d) and 1(l), original images divided by estimated inhomogeneity fields) eliminated most of inhomogeneity. For M3-4, outlines of single rectangular regions were used as initial curve. By careful setting of the position of initial curve, right result can be reached on $S1$ (Fig. 1(g)1(i)). However, the same initial curve leads to erroneous result in $S2$ (Fig. 1(o)1(q)), and intensity inhomogeneity is only partially corrected by N3(the underlying image of Fig. 1(i) and 1(q)).

For quantitative analysis, we manually segmented 10 axial slices evenly spaced in the tested dataset as gold standard, each automated method (M1-M4) is with fixed parameters and initial conditions mentioned above for segmentation of all these slices. If a pixel is classified by both manual and an automated method as muscle, it's considered as true positive. If it's classified as fat by manual method but as muscle by automated method, it's considered as false positive, etc. Since M1 didn't achieve any visually acceptable result in all slices, we only compared the sensitivity/accuracy/specificity of M2, M3 and M4 and the results are listed in Table I.

The quantitative results shows our method performs better than M3 and M4 in terms of sensitivity and accuracy, and is tied with them in term of specificity. However, the results of M3 and M4 were reached after many trial and error attempts since they are very sensitive to the position of initial curve and the parameters (especially the α value). To the contrary, our method only needs to tune the size of the initial squares to change result.

V. CONCLUSIONS AND FUTURE WORKS

In this paper, a generative image model is presented. Under this model, image segmentation and IC can be performed jointly, by the level set based active contour method. Testing result shows the effectiveness of the proposed model.

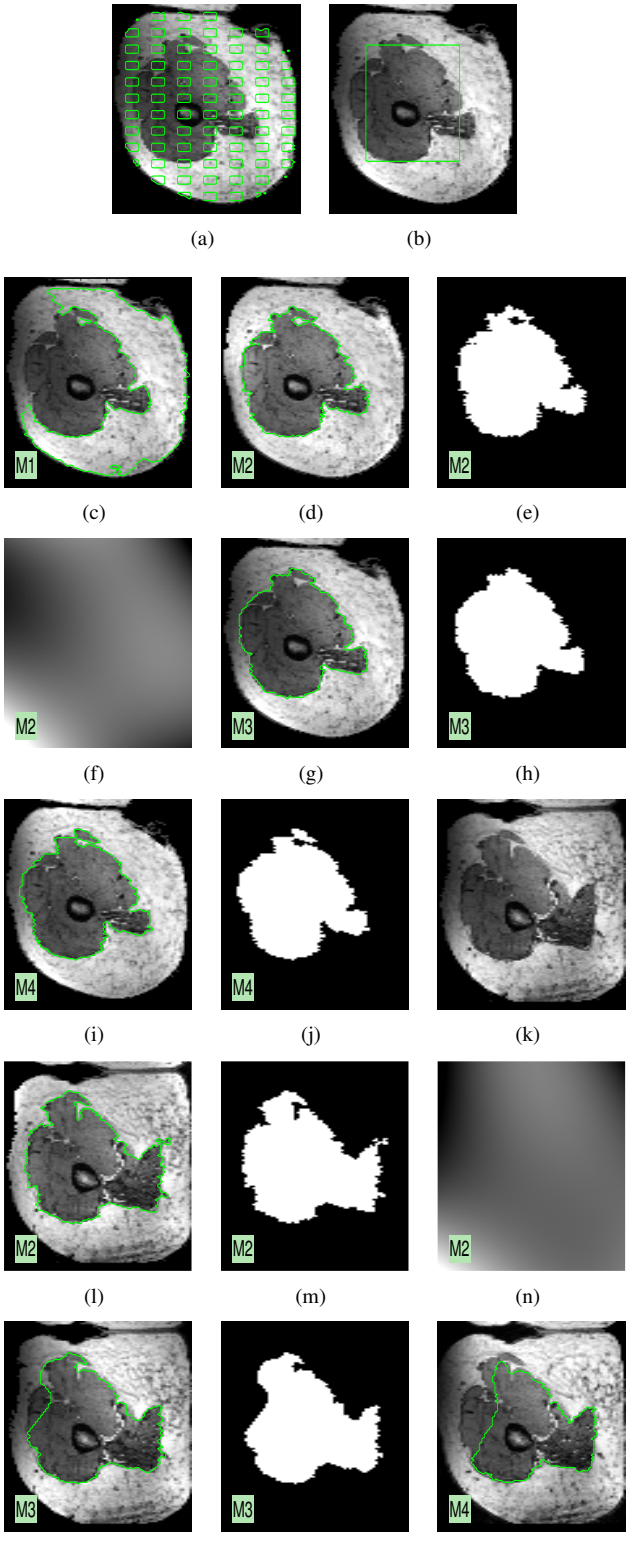

Fig. 1. Results of 4 methods on two slices named $S1$ and $S2$. 1(a): initial curve (green in the figure)position of M1 and M2 with underlying $S1$; 1(b): initial curve position of M3 and M4; 1(c): result of M1 on $S1$ with the final curve green; 1(d): result of M2 on $S1$ with original image corrected by estimated inhomogeneity field; 1(e), 1(f): binary mask and estimated inhomogeneity field by M2 on $S1$; 1(g) - 1(j): segmentation results of M3 and M4 on $S1$ with the underlying images of 1(i) corrected by N3; 1(k): original $S2$; 1(l) - 1(q): segmentation results on $S2$ by M2, M3 and M4;

Active contour based segmentation is not the only way that involves both the intensity values and geometric connectness between pixels. Interesting reports that do segmentation and IC jointly using Markov Random Field (MRF) theory can be found in [15], [16].

Future work includes incorporating prior shape knowledge for segmenting image with even weaker organ boundaries. And testing our method on MR images of other parts of body.

REFERENCES

[1] B. Johnston, M. Atkins, B. Mackiewich, and M. Anderson, "Segmentation of multiple sclerosis lesions in intensity corrected multispectral mri," *Medical Imaging, IEEE Transactions on*, vol. 15, no. 2, pp. 154 –169, Apr. 1996.

[2] L. Axel, J. Costantini, and J. Listerud, "Intensity correction in surface-coil mr imaging," *Am. J. Roentgenol.*, vol. 148, no. 2, pp. 418–420, 1987.

[3] I. Wells, W.M., W. Grimson, R. Kikinis, and F. Jolesz, "Adaptive segmentation of mri data," *Medical Imaging, IEEE Transactions on*, vol. 15, no. 4, pp. 429 –442, Aug. 1996.

[4] A. H. Andersen, Z. Zhang, M. J. Avison, and D. M. Gash, "Automated segmentation of multispectral brain mr images," *Journal of Neuroscience Methods*, vol. 122, no. 1, pp. 13 – 23, 2002.

[5] J. Ashburner and K. J. Friston, "Unified segmentation," *NeuroImage*, vol. 26, no. 3, pp. 839 – 851, 2005.

[6] J. Sled, A. Zijdenbos, and A. Evans, "A nonparametric method for automatic correction of intensity nonuniformity in MRI data," *Medical Imaging, IEEE Transactions on*, vol. 17, no. 1, pp. 87 –97, 1998.

[7] M. Kass, A. Witkin, and D. Terzopoulos, "Snakes: Active contour models," *International Journal of Computer Vision*, vol. 1, pp. 321–331, 1988, 10.1007/BF00133570.

[8] D. Mumford and J. Shah, "Optimal approximations by piecewise smooth functions and associated variational problems," *Communications on Pure and Applied Mathematics*, vol. 42, no. 5, pp. 577–685, 1989.

[9] J. A. Sethian, *Level Set Methods and Fast Marching Methods: Evolving Interfaces in Computational Geometry, Fluid Mechanics, Computer Vision, and Materials Science*, 2nd ed. Cambridge University Press, June 1999.

[10] T. Chan and L. Vese, "Active contours without edges," *Image Processing, IEEE Transactions on*, vol. 10, no. 2, pp. 266 –277, Feb. 2001.

[11] A. Tsai, J. Yezzi, A., and A. Willsky, "Curve evolution implementation of the Mumford-Shah functional for image segmentation, denoising, interpolation, and magnification," *Image Processing, IEEE Transactions on*, vol. 10, no. 8, pp. 1169 –1186, Aug. 2001.

[12] A. Tsai, A. J. Yezzi, and A. Willsky, "A curve evolution approach to smoothing and segmentation using the mumford-shah functional," in *Computer Vision and Pattern Recognition, 2000. Proceedings. IEEE Conference on*, 2000.

[13] U. Vovk, F. Pernus, and B. Likar, "A review of methods for correction of intensity inhomogeneity in mri," *Medical Imaging, IEEE Transactions on*, vol. 26, no. 3, pp. 405 –421, 2007.

[14] N. Tustison and J. Gee, "N4ITK: Nick's N3 ITK Implementation For MRI Bias Field Correction," *the Insight Journal*, Jan-Jun 2009.

[15] J. C. Rajapakse and F. Kruggel, "Segmentation of mr images with intensity inhomogeneities," *Image and Vision Computing*, vol. 16, no. 3, pp. 165 – 180, 1998.

[16] Y. Zhang, M. Brady, and S. Smith, "Segmentation of brain mr images through a hidden markov random field model and the expectation-maximization algorithm," *Medical Imaging, IEEE Transactions on*, vol. 20, no. 1, pp. 45 –57, Jan. 2001.